NASA-CR-202199

DEPARTMENT OF MECHANICAL ENGINEERING
COLLEGE OF ENGINEERING & TECHNOLOGY
OLD DOMINION UNIVERSITY
NORFOLK, VIRGINIA 23529

NONLINEAR STABILITY OF SUPERSONIC JETS

By

T.R.S. Bhat, Research Associate
and
Dr. S.N. Tiwari, Principal Investigator

Final Report
For the period ended May 31, 1996

September 1996

FOREWORD

This is a final report on the research project, "Instability Wave Models and Supersonic Jet Noise." The report titled "The Effects of Velocity Profiles on Supersonic Jet Noise" presented some of the earlier work done on this research project and, therefore, is not repeated here. Recent research activities were directed in the area of "Nonlinear Stability of Supersonic Jets."

NONLINEAR STABILITY OF SUPERSONIC JETS

T. R. S. Bhat[†] and S. N. Tiwari[§]
Department of Mechanical Engineering
Old Dominion University, Norfolk, VA 23529-0247

ABSTRACT

The stability calculations made for a shock-free supersonic jet using the model based on parabolized stability equations are presented. In this analysis the large-scale structures, which play a dominant role in the mixing as well as the noise radiated, are modeled as instability waves. This model takes into consideration non-parallel flow effects and also nonlinear interaction of the instability waves. The stability calculations have been performed for different frequencies and mode numbers over a range of jet operating temperatures. Comparisons are made, where appropriate, with the solutions to Rayleigh's equation (linear, inviscid analysis with the assumption of parallel flow). The comparison of the solutions obtained using the two approaches show very good agreement.

† Research Associate
§ Eminent Professor

TABLE OF CONTENTS

LIST OF FIGURES

LIST OF SYMBOLS

A, B	Coefficient matrices
C, D	Coefficient matrices
b	Half-width of the shear layer
f	Frequency in cycles/sec
h	Radius of the core region
M_x	Local Mach number
m	Mode number associated with frequency
n	Azimuthal mode number
p	Pressure
$\hat{p}$	Pressure eigenfunction
(r, θ, x)	Cylindrical coordinate system
R	Radius
St	Strouhal number, $2fR/W$
u	Radial velocity component
$\hat{u}$	Radial velocity eigenfunction
v	Azimuthal velocity component
$\hat{v}$	Azimuthal velocity eigenfunction
w	Axial velocity component
$\hat{w}$	Axial velocity eigenfunction
W	Mean axial velocity
V_{xx}, V_{xr}	Coefficient matrices
$V_{rr}, V_{r\theta}$	Coefficient matrices
$V_{\theta x}, V_{\theta\theta}$	Coefficient matrices

Greek Symbols

α	Axial wavenumber or eigenvalue
χ	Wave-like part
γ	Ratio of specific heats
Γ	Coefficient matrix
ϕ	Disturbance vector, $(\rho', u', v', w', p')^T$
Ψ	Shape function vector, $(\hat{\rho}, \hat{u}, \hat{v}, \hat{w}, \hat{p})^T$
ρ	Density
$\hat{\rho}$	Density eigenfunction

ω Angular frequency

Superscripts

$*$	Complex conjugate
$\prime$	Perturbation quantity
l	Linear part of the coefficient matrix
n	Nonlinear part of the coefficient matrix

Subscripts

m	Mode number index associated with frequency
n	Azimuthal mode number index

1. INTRODUCTION

The aerospace engineering community has placed a major emphasis on the development of a high speed civil transport aircraft. The success of this effort hinges on several factors. One of the major problems that needs to be addressed is the environmental issue of the noise generated by aircraft at take-off, cutback, and approach engine power settings. Jet noise represents a significant percentage of the overall noise generated. Hence, the reduction of jet noise is of utmost importance to future development of a supersonic civil aircraft. This has led to a revival of interest in developing techniques to predict and ultimately suppress noise radiated by supersonic jets.

Several approaches have been developed for the prediction of jet noise. One such approach is the direct numerical simulation of the full Navier-Stokes equations for the estimation of the radiated noise. This technique, although exact, is not practical because of the requirements of the computational resources. This has led to development of models based on simplified governing equations. Mankbadi et al.[1] developed such a technique by using large-eddy simulation to model the flow field and calculated the far-field noise by applying Lighthill's acoustic analogy. These techniques also require extensive computational power. Recently, there has been lot of focus on extending computational fluid dynamics techniques for aeroacoustic applications. The development of these techniques are not simple as the requirements on numerical dissipation, dispersion, etc. for acoustic analysis are very rigid, see Tam[2].

A different approach for the prediction of jet noise is based on combining theoretical and analytical methods. It is well established that turbulent flows possess coherent large-scale structures. These structures control the turbulent mixing process and also play a dominant role in the noise generation process. It has been successfully shown, in free shear layers such as plane mixing layers and jets, that the large-scale motions can be modeled as a random superposition of instability waves. The noise generated by these waves compare well with the experimental data. A good review of this approach is presented in Tam[3]. This model can be used to determine the two important characteristics of an instability wave, phase velocity and growth rate, which determine the mixing as well as the noise radiated.

Most of the earlier theoretical studies of supersonic jets have considered linear,

inviscid analysis and have assumed the mean flow to be parallel. Tam and Burton[4] took into consideration the non-parallel flow effects by using the method of multiple-scales. The real physical process of jets involve nonlinear interaction among all turbulence scales. The nonlinearities considered in this paper may be divided into nonlinear interaction between the instability waves and the mean flow, and the nonlinear self interaction of the instability waves. The former leads to a change in the mean-flow distribution, which in turn will modify the axial development of the instability waves. This kind of nonlinear effect can be taken into account by using measured mean velocity data. However, this data is not always readily available for different flow conditions. The effects of nonlinear self-interaction of the instability waves have been neglected in all the earlier studies by assuming that the amplitude of the disturbances, which initiate the instability waves near the nozzle exit, are small. This assumption may not be valid in all cases.

In this study, nonlinear stability analysis of supersonic jets is considered. This analysis also accounts for non-parallel flows. The nonlinear interaction of the waves are predicted by the solving the parabolized stability equations (PSE). Bertoloti et al.[5] and Chang et al.[6] have applied PSE based technique for the stability analysis of incompressible and compressible boundary layers. The mean flow varies slowly in the axial direction enabling one to decompose the perturbation quantities into a rapidly varying wave-like part and a slowly varying shape function. The PSE can then be derived from the Navier-Stokes equations by applying parabolizing approximation to the shape function. The simplified governing equations can be solved by marching along the streamwise direction. This method is not computationally expensive.

In this report stability calculations of supersonic jets using the PSE are presented. The calculations have been performed for different frequencies and mode numbers over a range of jet temperatures, from cold to hot. In section 2, the development of the PSE model is presented and in section 3 computational procedure is described. The numerical results obtained for different cases are presented in section 4. Finally, in section 5, a summary of the results is given and also ways of improving the model and plans for future work are discussed.

2. ANALYSIS

Consider the development of instability waves generated in a shock-free jet. It is assumed that the instability waves are governed by the compressible equations of motion, energy and state for a perfect gas. The flow variables are decomposed into a mean value and a perturbation quantity

$$f(r, \theta, x, t) = \bar{f}(r, \theta, x) + f'(r, \theta, x, t) \qquad (2.1)$$

where f is any flow variable and (r, θ, x) is the polar coordinate system with x in the axial direction. The governing equations for the disturbances are obtained by substituting the form given by equation (2.1) in the governing equations and subtracting the equations for the mean flow. The resulting equations can be expressed as

$$\Gamma \frac{\partial \phi}{\partial t} + A \frac{\partial \phi}{\partial x} + B \frac{\partial \phi}{\partial \theta} + C \frac{\partial \phi}{\partial r} + D\phi = V_{xx} \frac{\partial^2 \phi}{\partial x^2} + V_{xr} \frac{\partial^2 \phi}{\partial x \partial r}$$
$$+ V_{rr} \frac{\partial^2 \phi}{\partial r^2} + V_{r\theta} \frac{\partial^2 \phi}{\partial r \partial \theta} + V_{\theta x} \frac{\partial^2 \phi}{\partial \theta \partial x} + V_{\theta\theta} \frac{\partial^2 \phi}{\partial \theta^2} \qquad (2.2)$$

where ϕ is the disturbance vector and is given by $\phi = (\rho', u', v', w', p')^T$. The coefficient matrices, $\Gamma, A, B, ..., V_{\theta x}$ and $V_{\theta\theta}$ are composed of a linear part and a nonlinear part. The linear part (denoted by superscripts l) contains only mean flow quantities and the nonlinear part (denoted by superscripts n) contains disturbance quantities , i.e. $\Gamma = \Gamma^l + \Gamma^n$, etc. Equation (2.2) can then be rearranged as

$$\Gamma^l \frac{\partial \phi}{\partial t} + A^l \frac{\partial \phi}{\partial x} + B^l \frac{\partial \phi}{\partial \theta} + C^l \frac{\partial \phi}{\partial r} + D^l \phi - V_{xx}^l \frac{\partial^2 \phi}{\partial x^2}$$
$$- V_{xr}^l \frac{\partial^2 \phi}{\partial x \partial r} - V_{rr}^l \frac{\partial^2 \phi}{\partial r^2} - V_{r\theta}^l \frac{\partial^2 \phi}{\partial r \partial \theta} - V_{\theta x}^l \frac{\partial^2 \phi}{\partial \theta \partial x}$$
$$- V_{\theta\theta}^l \frac{\partial^2 \phi}{\partial \theta^2} = F^n \qquad (2.3)$$

where F^n includes all nonlinear interaction terms associated with the disturbances and is given by

$$F^n = -\Gamma^n \frac{\partial \phi}{\partial t} - A^n \frac{\partial \phi}{\partial x} - B^n \frac{\partial \phi}{\partial \theta} - C^n \frac{\partial \phi}{\partial r} - D^n \phi$$
$$+ V_{xx}^n \frac{\partial^2 \phi}{\partial x^2} + V_{xr}^n \frac{\partial^2 \phi}{\partial x \partial r} + V_{rr}^n \frac{\partial^2 \phi}{\partial r^2} + V_{r\theta}^n \frac{\partial^2 \phi}{\partial r \partial \theta} + V_{\theta x}^n \frac{\partial^2 \phi}{\partial \theta \partial x}$$
$$+ V_{\theta\theta}^n \frac{\partial^2 \phi}{\partial \theta^2} \qquad (2.4)$$

The governing equations (2.3) have to be parabolized to enable a marching solution in the streamwise direction. This is accomplished by decomposing the disturbances into a rapidly varying wave-like part and a slowly varying shape function. The wave part retains its ellipticity while the governing equations for the shape function are parabolized. We assume that the disturbance vector ϕ for an instability wave with a frequency $m\omega$ and azimuthal mode number n can be expressed as

$$\phi(r,\theta,x,t) = \sum_{m=-\infty}^{m=\infty} \sum_{n=-\infty}^{n=\infty} \Psi_{mn}(r,x)\chi_{mn}(\theta,x,t) \tag{2.5}$$

where the wave-like part χ_{mn} is given by

$$\chi_{mn} = \exp\left\{ i\left[\int_{x_o}^{x} \alpha_{mn}(\xi)d\xi + n\theta - m\omega t \right] \right\} \tag{2.6}$$

α_{mn} is the axial wavenumber and Ψ_{mn} is the shape function vector given by $\Psi_{mn} = (\hat{\rho}, \hat{u}, \hat{v}, \hat{w}, \hat{p})^T$. As the shape function is assumed to vary slowly with the streamwise direction x, the second derivative $\partial^2 \Psi / \partial x^2$ is very small and is neglected. The governing equations for the shape function of a single mode (m,n), using the form given by equation (2.5), can then be written as

$$\hat{D}_{mn}\Psi_{mn} + \hat{A}_{mn}\frac{\partial \Psi_{mn}}{\partial x} + \hat{C}_{mn}\frac{\partial \Psi_{mn}}{\partial r} = V_{rr}^l \frac{\partial^2 \Psi_{mn}}{\partial r^2}$$
$$+ \hat{F}_{mn}/\mathcal{A}_{mn} \tag{2.7}$$

where

$$\mathcal{A}_{mn} = \exp\left[i\int_{x_o}^{x} \alpha_{mn}(\xi)d\xi \right]$$

The nonlinear forcing function $\hat{F}_{mn}$ can be evaluated from the Fourier series expansion of F^n

$$F^n(r,\theta,x,t) = \sum_{m=-\infty}^{m=\infty} \sum_{n=-\infty}^{n=\infty} \hat{F}_{mn} \exp\left[i(n\theta - m\omega t) \right] \tag{2.8}$$

In equation (2.7), the elliptic effect associated with the wave part is absorbed in matrices $\hat{D}, \hat{A}$ and $\hat{C}$ and does not contribute to the upstream influence. However, the term $\partial\hat{p}/\partial x$ allows upstream influence in subsonic regions of the flow. In order to make equation (2.7) truly parabolic, $\partial\hat{p}/\partial x$ is multipled by a constant Ω given by

$$\Omega = \begin{cases} \frac{\gamma M_x^2}{1+(\gamma-1)M_x^2}, & M_x < 1 \\ 1 & M_x \geq 1 \end{cases} \tag{2.9}$$

where M_x is the local Mach number. This parabolizing procedure yield solutions for the parabolized Navier-Stokes equations which compare well with those obtained by the full Navier-Stokes equations, see Rubin[7].

3. NUMERICAL SCHEME

The parabolized stability equation (2.7) is solved numerically by finite-differencing the derivatives with respect to x and r. In the formulation given below, $\Psi_{i,j}$ represents the shape function with an axial location index i and radial location denoted by index j. The streamwise derivative at (i,j) is replaced by a second-order backward difference given by

$$\frac{\partial \Psi}{\partial x} = (3\Psi_{i,j} - 4\Psi_{i-1,j} + \Psi_{i-2,j})/2\Delta x \qquad (3.1)$$

for all axial locations except for the starting plane where a first-order backward differencing is used. The resulting discretized equation for the i-th axial plane is

$$\left[\hat{D} + \frac{3}{2\Delta x}\hat{A} + \hat{C}\frac{\partial}{\partial r} - V_{rr}^{l}\frac{\partial^2}{\partial r^2} \right]_{i,j} \Psi_{i,j} = \hat{A}_{i,j}(4\Psi_{i-1,j} - \Psi_{i-2,j})/2\Delta x + \hat{F}/\mathcal{A} \quad (3.2)$$

where for convenience, the subscript mn which identifies the mode (m,n) is dropped. The radial derivatives are discretized using a fourth-order central differencing and are given by

$$\frac{\partial \Psi}{\partial r} = \frac{-\Psi_{i,j+2} + 8\Psi_{i,j+1} - 8\Psi_{i,j-1} + \Psi_{i,j-2}}{12\Delta r} \qquad (3.3)$$

$$\frac{\partial^2 \Psi}{\partial r^2} = \frac{-\Psi_{i,j+2} + 16\Psi_{i,j+1} - 30\Psi_{i,j} + 16\Psi_{i,j-1} - \Psi_{i,j-2}}{12\Delta r^2} \qquad (3.4)$$

The above finite differencing scheme is replaced by a second-order scheme for the grid point next to the boundary. The second-order scheme can be written as

$$\frac{\partial \Psi}{\partial r} = (\Psi_{i,j+1} - \Psi_{i,j+1})/2\Delta r \qquad (3.5)$$

$$\frac{\partial^2 \Psi}{\partial r^2} = (\Psi_{i,j+1} - 2\Psi_{i,j} + \Psi_{i,j-1})/2\Delta r^2 \qquad (3.6)$$

The finite difference formulations given above are substituted into equation (2.7). This coupled with the boundary conditions results in a block penta-diagonal system of equations (block size of 5 x 5) at each axial location for the unknown shape functions, Ψ_{mn}.

The boundary conditions have to be prescribed for the eigenfunctions at the jet centerline and at a radial location of infinity. As the governing equations become

singular at $r = 0$, L'Hospital's rule is applied at the centerline to obtain a new set of governing equations. The boundary conditions along the centerline takes a different form based on the azimuthal mode number. For example, for axisymmetric mode, i.e. $n = 0$, the boundary conditions at $r = 0$ are given by

$$\hat{u} = \hat{v} = 0, \quad \partial \hat{w} / \partial r = \partial \hat{p} / \partial r = 0 \tag{3.7}$$

Here, the velocity components $\hat{u}, \hat{v}, \hat{w}$ are in the r, θ, x directions, respectively. The boundary condition on density is obtained from (3.7) and the discretized continuity equation. At the outer boundary, far from the centerline, all the shape functions are set equal to zero. For the nonlinear analysis, the far-field boundary conditions can be directly applied for all modes except for modes with zero frequency ($m = 0$) and axisymmetric mode ($n = 0$). The case of $m = 0$ and $n = 0$ is referred to as the mean flow correction mode. For this mode, the condition $\hat{u} = 0$ is replaced by $\partial \hat{u} / \partial r = 0$.

The solution procedure is as follows: start with a known solution for α_{mn} and Ψ_{mn} at $x = x_0$, assume a value for α_{mn} at the next axial location, march the PSE to the next station by solving for Ψ_{mn}. The new value of α_{mn} is determined from

$$\alpha_{mn, \, new} = \alpha_{mn, \, old} - \frac{i}{\Psi_{mn}} \frac{d\Psi_{mn}}{dx} \tag{3.8}$$

and this process is repeated until the difference between the assumed and computed values of α_{mn} is less than a given tolerance. The updating procedure given above is equivalent to normalizing the shape function such that $d\Psi/dx$ is zero at a particular radial location. As the shape function vector Ψ is a function of r and contains five dependent variables, there is no unique wavenumber as in the liner theory for parallel flows. However, as shown by Chang et al.[6], the total growth rate appears to be very weakly dependent upon the normalization. Further details of the normalization and its effect on the computed wavenumber are given in Chang et al.[6]. In all the results presented here, we have chosen to compute the wavenumber based on streamwise velocity using

$$\alpha_{mn, \, new} = \alpha_{mn, \, old} - i \frac{\int_0^\infty \hat{u}^* \partial \hat{u} / \partial x \, dr}{\int_0^\infty | \hat{u} |^2 \, dr} \tag{3.9}$$

where $*$ denotes complex conjugate.

4. NUMERICAL RESULTS

The PSE has been used to analyze the linear stability of a supersonic jet issuing from a circular nozzle operating at design Mach number of 2.0. It has been assumed that the axial evolution of the instability waves can be treated as an inviscid phenomena and $\hat{F}_{mn}$ in equation (2.7) is zero. The results obtained for parallel flows using the PSE are compared with the solutions to equation governing linear, inviscid instability wave, i.e., the compressible Rayleigh's equation. The solutions to the Rayleigh's equation (RES) are obtained using the method of Seiner, Bhat and Ponton[8]. For both the approaches, i.e., PSE and RES, the mean flow field is assumed to be known. It has been shown that the mean velocity profile can be closely approximated by a half-Gaussian function given by

$$W(x) = \begin{cases} W_c(x) & r \leq h \\ W_c(x)\exp[-\ln 2(r-h)/b^2] & r > h \end{cases} \qquad (4.1)$$

where $h(x)$ is the radius of the potential core, $b(x)$ is the half-width of the shear layer and $W_c(x)$ is the jet centerline velocity. For the present calculations, the values of these parameters are obtained from computational data of Viswanathan et al.[9].

Calculations have been performed for a range of frequencies and the modes considered are $n = 0$, the axisymmetric mode, $n = 1$ and 2, the helical modes. These calculations were carried out over a range of jet operating temperatures. However, for conciseness, the results for $n = 1$ mode are shown here for a cold jet. The two most important characteristics of an instability wave are the phase velocity and growth rate. The phase velocity is defined as as $2\pi f/\alpha_r$ where f is the frequency and α_r is the real part of the complex wavenumber α. The growth rate is defined as $-\alpha_i$ where α_i is the imaginary part of the wavenumber. Figures 1 and 2 compare the phase velocity and growth rates obtained using the two approaches at two different axial locations. It can be seen that over the entire range of Strouhal number $(St = 2fr_j/W_j)$ considered, the two solutions are in very good agreement. Similar agreements are also obtained for $n = 0$ and 2. Figures 3 and 4 show the comparison as a function of downstream distance for axisymmetric mode ($n = 0$) at $St = 0.54$ and the helical mode ($n = 1$) at $St = 0.49$. Once again, the agreement is excellent for both the phase velocity and growth rate. As mentioned

before, calculations have also been performed for hot jets obtaining good agreement between the solutions using the two approaches.

The results presented so far have been obtained for parallel flows. We now consider the solution of linear PSE with non-parallel flow effects. As in any marching scheme, an initial solution is needed to start the computations. To provide a good starting solution, the multiple-scales analysis can be used which accounts for non-parallel flow effects. It has been shown by Chang et al.[6] that using any incorrect initial conditions result in a transient phenomena close to the jet exit. Furthermore, it was observed that the PSE approach is capable of recovering the correct solution in the marching process provided the input initial conditions are close to the correct solution. In this study, the linear parallel stability equations are solved and the eigenvalue and eigenfunctions are used as the starting solutions.

The linear PSE with non-parallel flow effects have been solved for several cases. Figures 5 and 6 show the results for two of these cases. Once again, calculations are carried out for a cold supersonic jet operating at its design Mach number of 2.0. In figure 5, the variation of the wavenumber (real part) and the growth rate with axial distance is presented for axisymmetric mode ($n = 0$) at $St = 0.54$. The results from parallel stability theory are included for comparison. As can be seen, the wavenumber and the growth rates start off being less than those based on parallel theory. After some initial transients, both the wavenumber and growth rate are larger than those from parallel theory. This implies that the wave based on non-parallel flow has a lower phase velocity than the wave based on parallel flow. In addition, the wave corresponding to the non-parallel flow gets damped further downstream than that obtained using parallel flow assumption. The results for helical mode ($n = 1$) at $St = 0.49$ are presented in figure 6. Similar trends as in axisymmetric mode are observed. The only difference is that the wavenumber based on parallel and non-parallel mean flow are more or less the same.

The eigenfunction distribution for the cases discussed above are presented next. Figure 7 shows the radial distributions of the eigenfunctions for the axisymmetric mode, $St = 0.54$ at $X/R_j = 0$. The eigenfunctions shown are the radial velocity component, $\hat{u}$, axial velocity component, $\hat{w}$, and pressure, $\hat{p}$. For this case, the azimuthal velocity component, $\hat{v}$, is zero. As can be seen, the axial velocity component is very large and peaks in the shear layer. These eigenfunctions further downstream, at $X/R_j = 10$, are presented in figure 8. The amplitude of the pressure eigenfunc-

tion has increased slightly while the amplitude of the axial velocity component has decreased substantially. The axial location for peak noise emission, based on the experimental observations of Troutt and McLaughlin[10] and Seiner, et al.[11], occurs near each wave's neutral point. This suggests that the amplitude of pressure would increase with downstream distance until the wave has become damped.

The eigenfunctions for $n = 1$, $St = 0.49$ at two axial locations, $X/R_j = 0$ and $X/R_j = 10$ are shown in figures 9 and 10, respectively. In this case, the azimuthal velocity component is nonzero. It can be seen that the trends are similar to that of the axisymmetric mode. The only difference is that the amplitude of the azimuthal velocity component, $\hat{v}$, has increased. Converged solutions to the nonlinear PSE could not be obtained. Currently, this problem is being investigated. Some of the possible reasons for not getting converged solutions are discussed in the next section.

5. DISCUSSIONS AND CONCLUSIONS

In this study, a model for linear and nonlinear stability analysis of supersonic jets is developed using the parabolized stability equations. The linear PSE has been used to analyze the instability waves of a supersonic jet operating at design conditions, i.e., shock-free. For parallel flows, it has been shown that the PSE approach and the solutions to Rayleigh's equation are in very good agreement over a range of frequencies and azimuthal mode numbers. The axial development of the instability waves also compared well. These calculations also considered a range of jet operating temperatures from cold to hot. The important characteristics of the instability waves, i.e., phase velocity and growth rate, are predicted well using the PSE.

The linear PSE model has also been used to study the non-parallel flow effects. The computed solutions show that the growth rate is higher and the wave's phase velocity is lower than that corresponding to the parallel flow. This expected trend is seen for instability waves of different frequencies and mode numbers. We have assumed that the dynamics of the axial development of the instability waves can be treated as an inviscid phenomena. At distances far downstream from the jet exit the instability wave would no longer grow in amplitude and is damped. At these locations the governing equations become singular and the integration contour must be deformed around the critical point, see Tam[12] and Tam and Morris[13]. In this study, the calculations are terminated close to the neutral point of the wave.

The results presented here are preliminary and is by no means complete. In order to improve this model, there are several issues that need to be investigated. First of all, the solutions obtained from linear parallel stability equations have been used as the initial conditions for the marching scheme. The sensitivity of the initial conditions to the converged solutions have to be studied. Solutions obtained using the multiple-scales analysis, which accounts for non-parallel flow effects, can be used as the initial conditions for the eigenvalue and the eigenfunctions. Secondly, to circumvent the problem associated with the damped inviscid wave and to study the effects of Reynolds number, viscous terms have to be included in the analysis.

As mentioned before, converged solutions to the nonlinear PSE could not be obtained. It appears that the initial amplitudes of the various waves considered play a critical role in getting converged solutions. Furthermore, the selection of the

waves, with nonzero initial amplitudes, also influences the iterative process. The effects of the initial amplitudes and the choice of the waves on getting converged solutions should also be investigated. The solutions obtained from nonlinear PSE analysis, after all the issues related to convergence have been identified and resolved, can be validated by comparing it to solutions computed from nonlinear numerical simulation, for example, the results of Viswanathan and Sankar[14].

REFERENCES

1. Mankbadi, R. R., Hayder, M. E. and Povinelli, L. A., " Structure of Supersonic Jet Flow and its Radiated Sound", AIAA Journal, Vol. 32, No. 5, 1994. pp. 897-906.

2. Tam, C. K. W., "Computational Aeroacoustics: Issues and Methods," AIAA Paper No. 95-0677.

3. Tam, C. K. W., "Jet Noise Generated by Large-Scale Coherent Motion", Aeroacoustics of Flight Vehicles: Theory and Practice, Vol. 1: Noise Sources, NASA RP-1258, 1991.

4. Tam, C. K. W. and Burton, D. E., "Sound Generated by Instability Waves of Supersonic Flows, Part I. Two-Dimensional Mixing Layers, Part II. Axisymmetric Jets", Journal of Fluid Mechanics, Vol. 138, 1984, pp. 249-295.

5. Bertolotti, F. P., Herbert, Th., and Spalart, P. R., "Linear and Nonlinear Stability of the Blasius Boundary Layer", Journal of Fluid Mechanics, Vol. 242, 1992, pp. 441-474.

6. Chang, Chau-Lyan, Malik, M. R., Erlebacher, G., and Hussaini, M. Y., "Linear and Nonlinear PSE for Compressible Boundary Layers", NASA Contractor Report 191537, Sep. 1993.

7. Rubin, S. G., "A Review of Marching Procedures for Parabolized Navier-Stokes Equations", Proceedings of Symposium on Numerical and Physical Aspects of Aerodynamic Flows, Springer-Verlag, 1981, pp. 171-186.

8. Seiner, J. M., Bhat, T. R. S. and Ponton, M. K., "Mach Wave Emission from a High Temperature Supersonic Jet", AIAA Journal, Vol. 32, No. 12, 1994, pp. 2345-2350.

9. Viswanathan, K., Sankar, L. N. and Reddy, N. N., "A Fluid/Acoustic Coupled Simulation of Supersonic Jet Noise", AIAA Paper No. 94-0137.

10. Troutt, T.R., and McLaughlin, D.K., "Experiments on the Flow and Acoustic Properties of a Moderate Reynolds Number Supersonic Jet", Journal of Fluid Mechanics, Vol. 116, Mar. 1982, pp. 123-156.

11. Seiner, J.M., McLaughlin, D.K., and Liu, C.H., "Supersonic Jet Noise Generated by Large Scale Instabilities", NASA TP-2072, Sep. 1982.

12. Tam, C. K. W., "Supersonic Jet Noise Generated by Large-Scale Disturbances", Journal of Sound and Vibration, Vol. 38, 1975, pp. 51-79.

13. Tam, C. K. W. and Morris, P. J., "The Radiation of Sound by the Instability Waves of a Compressible Plane Turbulent Shear Layer", Journal of Fluid Mechanics, Vol. 98, 1980, pp. 349-381.

14. Viswanathan, K. and Sankar, L. N., "Numerical Simulation of the Turbulence Structure of High Speed Jets", AIAA Paper No. 94-2192.
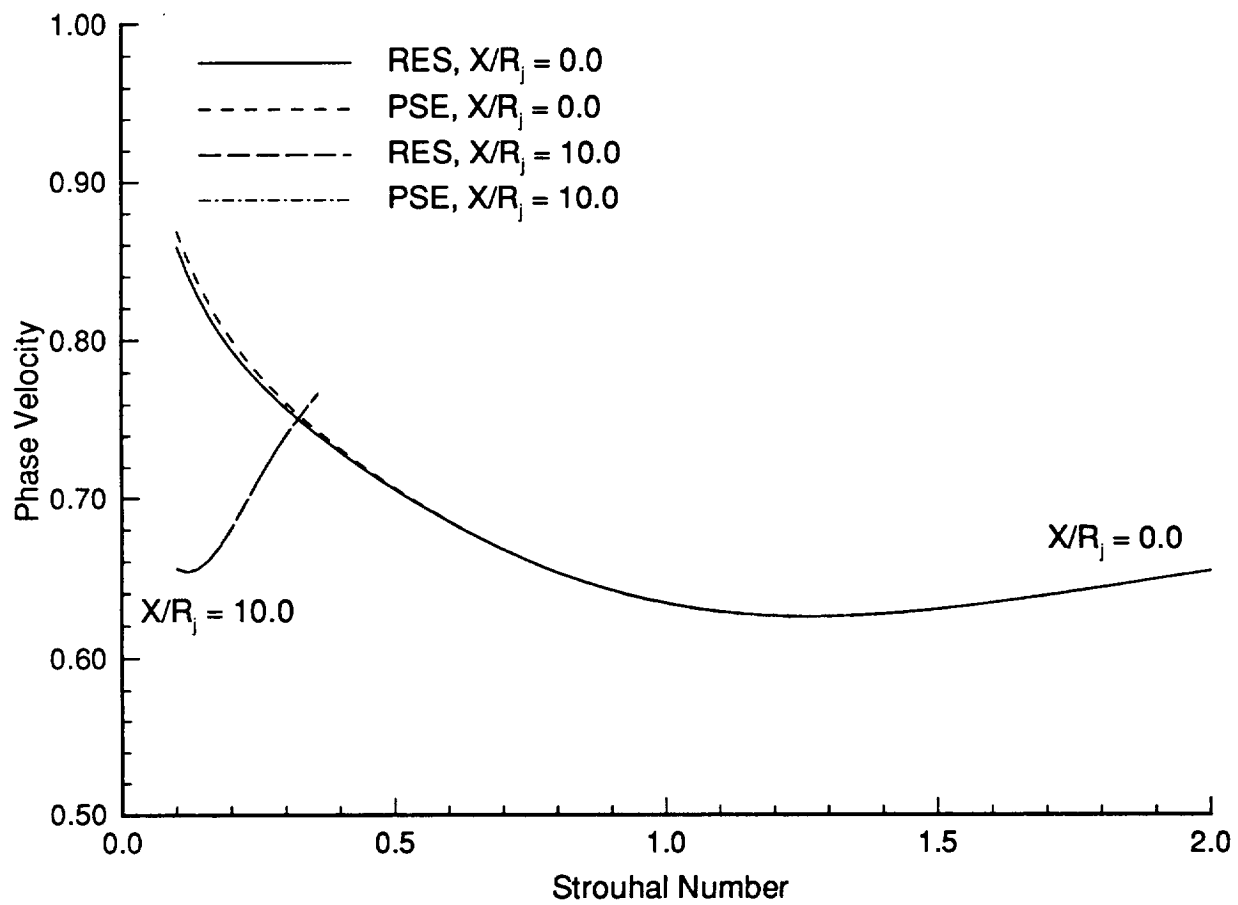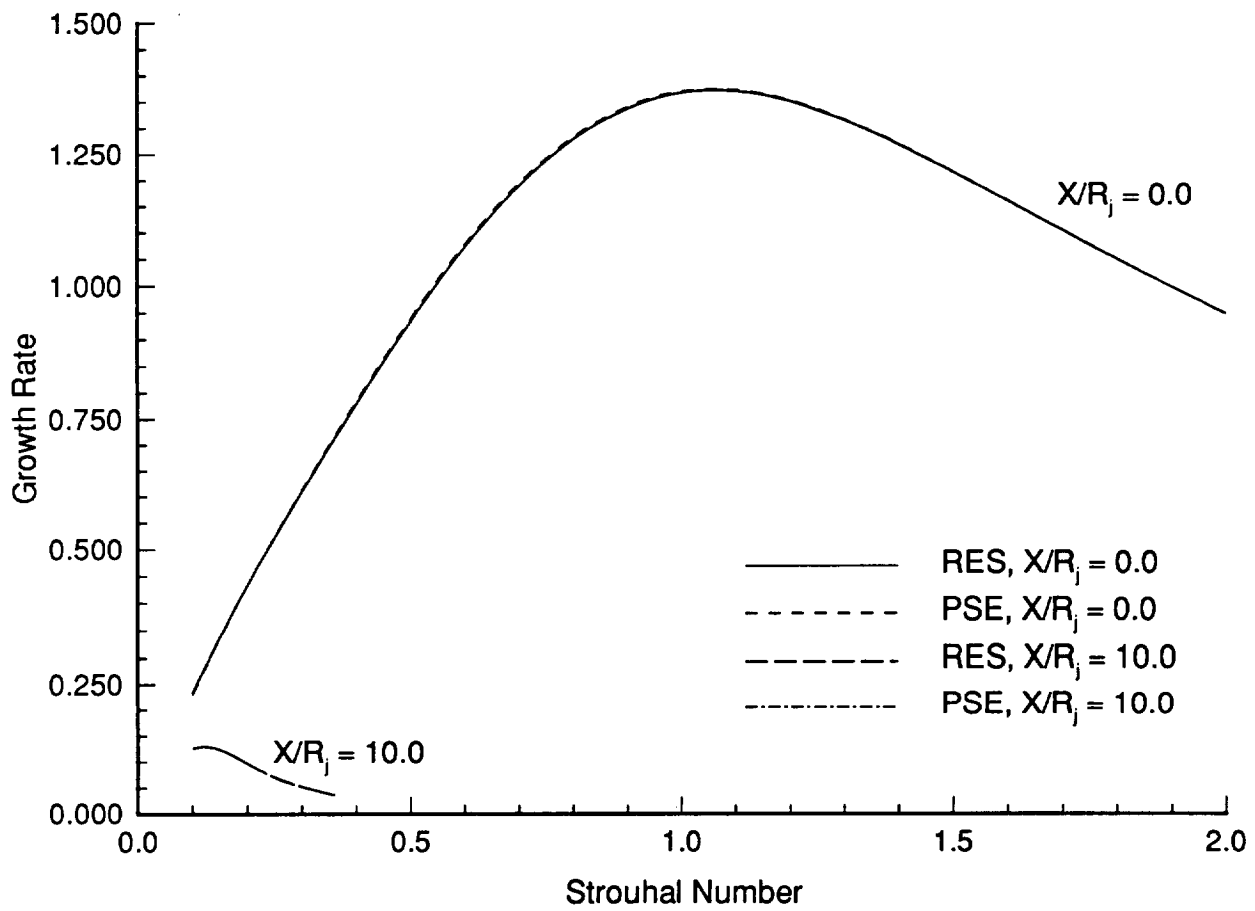
Fig. 1. Comparison of phase velocities.
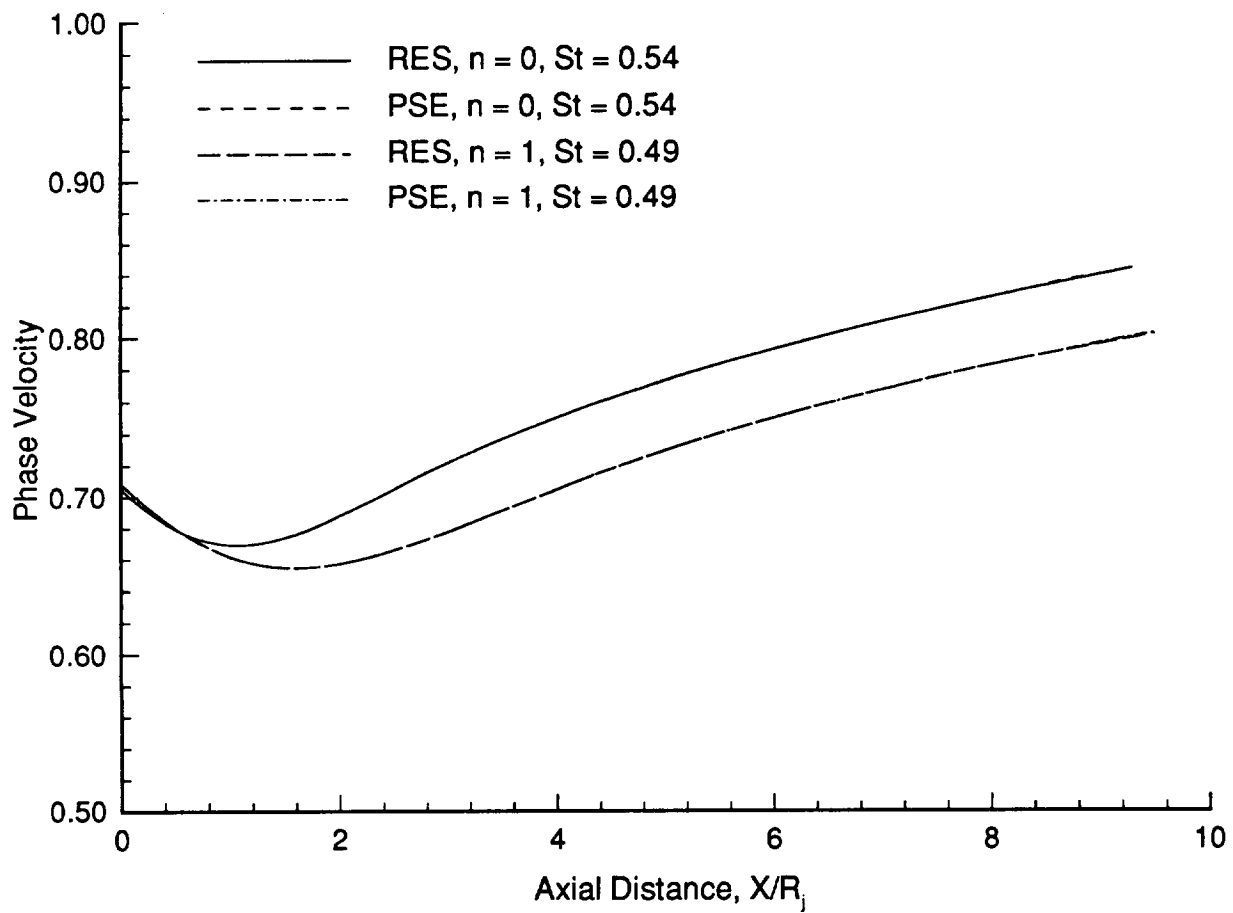
Fig. 2. Comparison of growth rates.
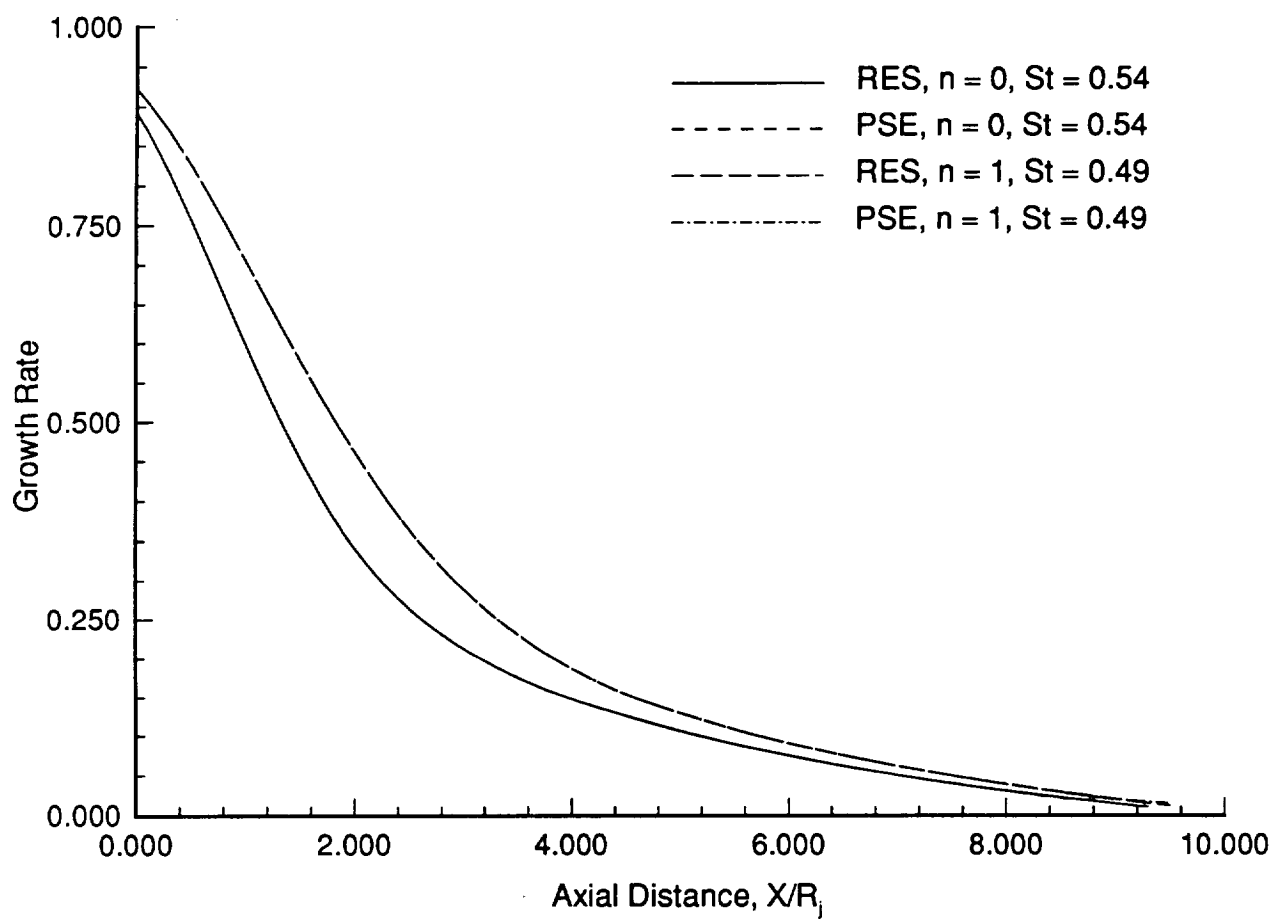
Fig. 3. Axial variation of phase velocities.

Fig. 4. Axial variation of growth rates.
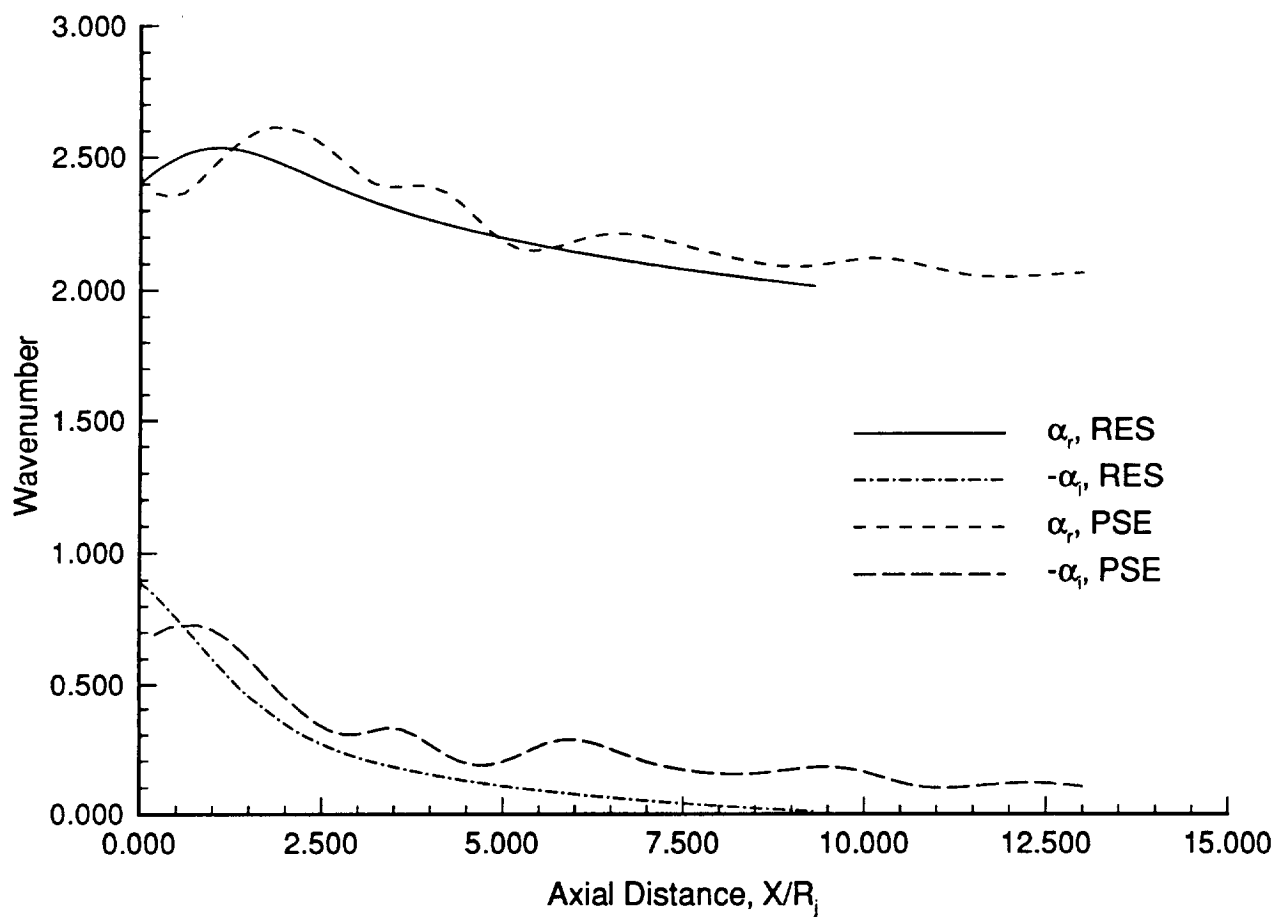
Fig. 5. Comparison of wavenumbers, $n = 0$, $St = 0.54$.
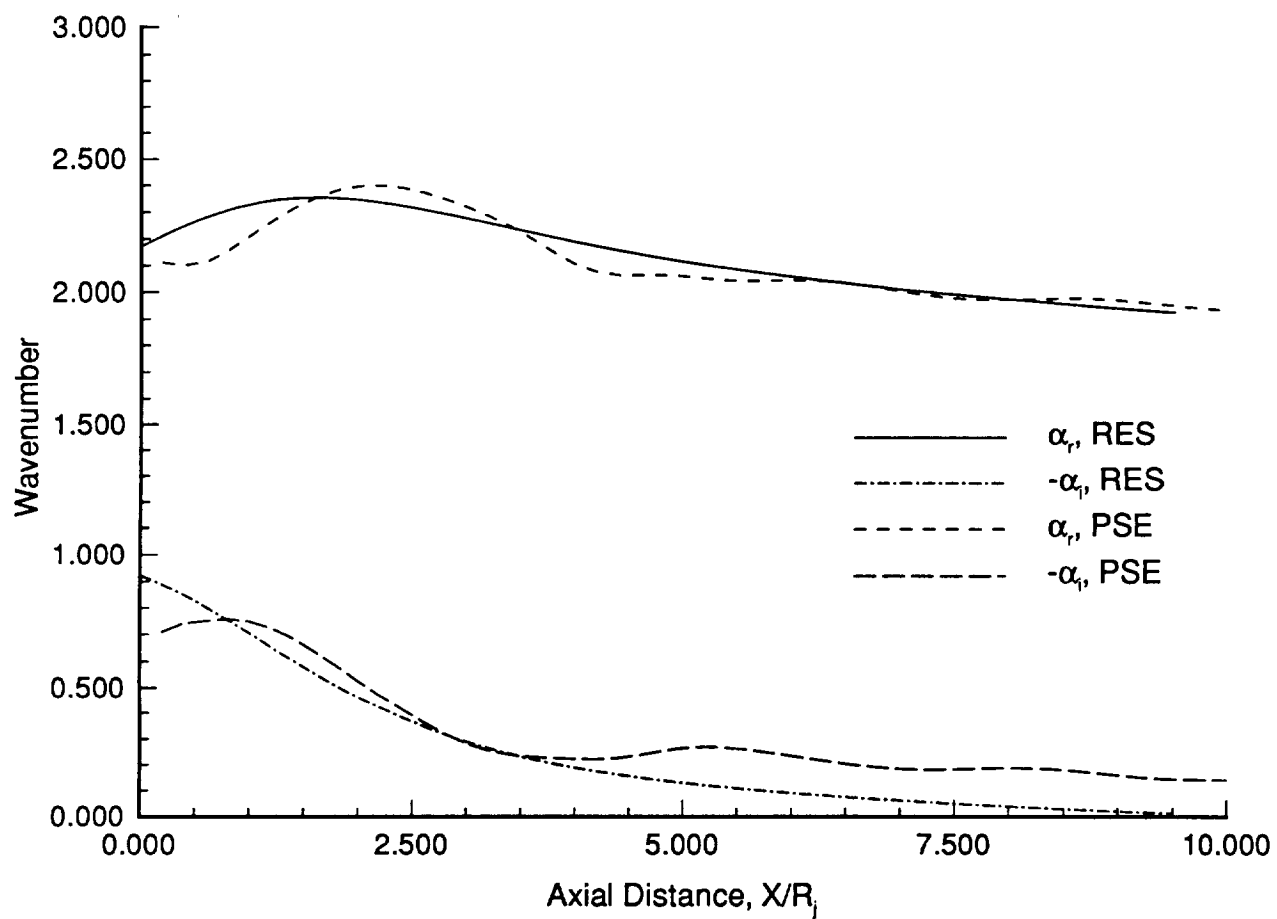
Fig. 6. Comparison of wavenumbers, $n = 1$, $St = 0.49$.
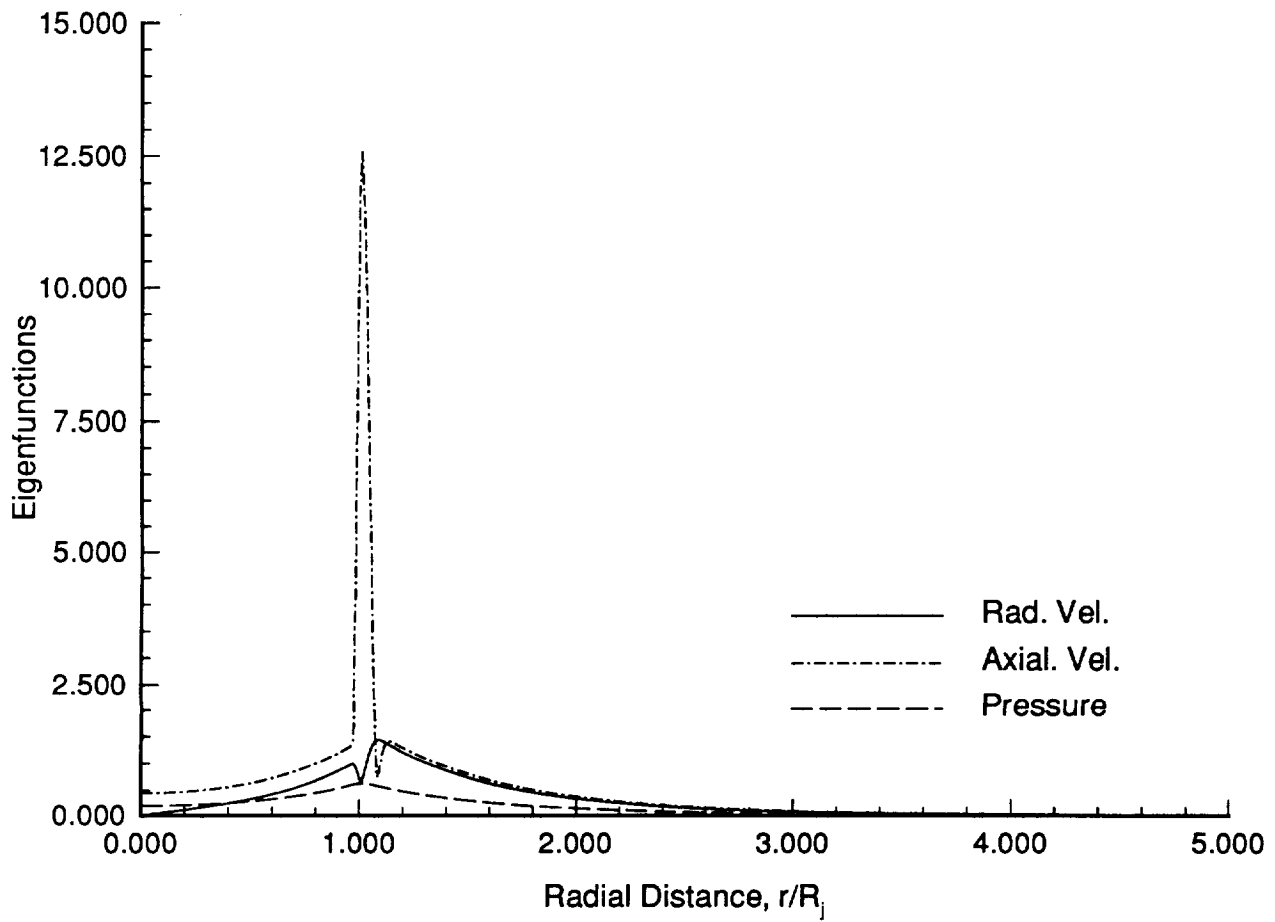
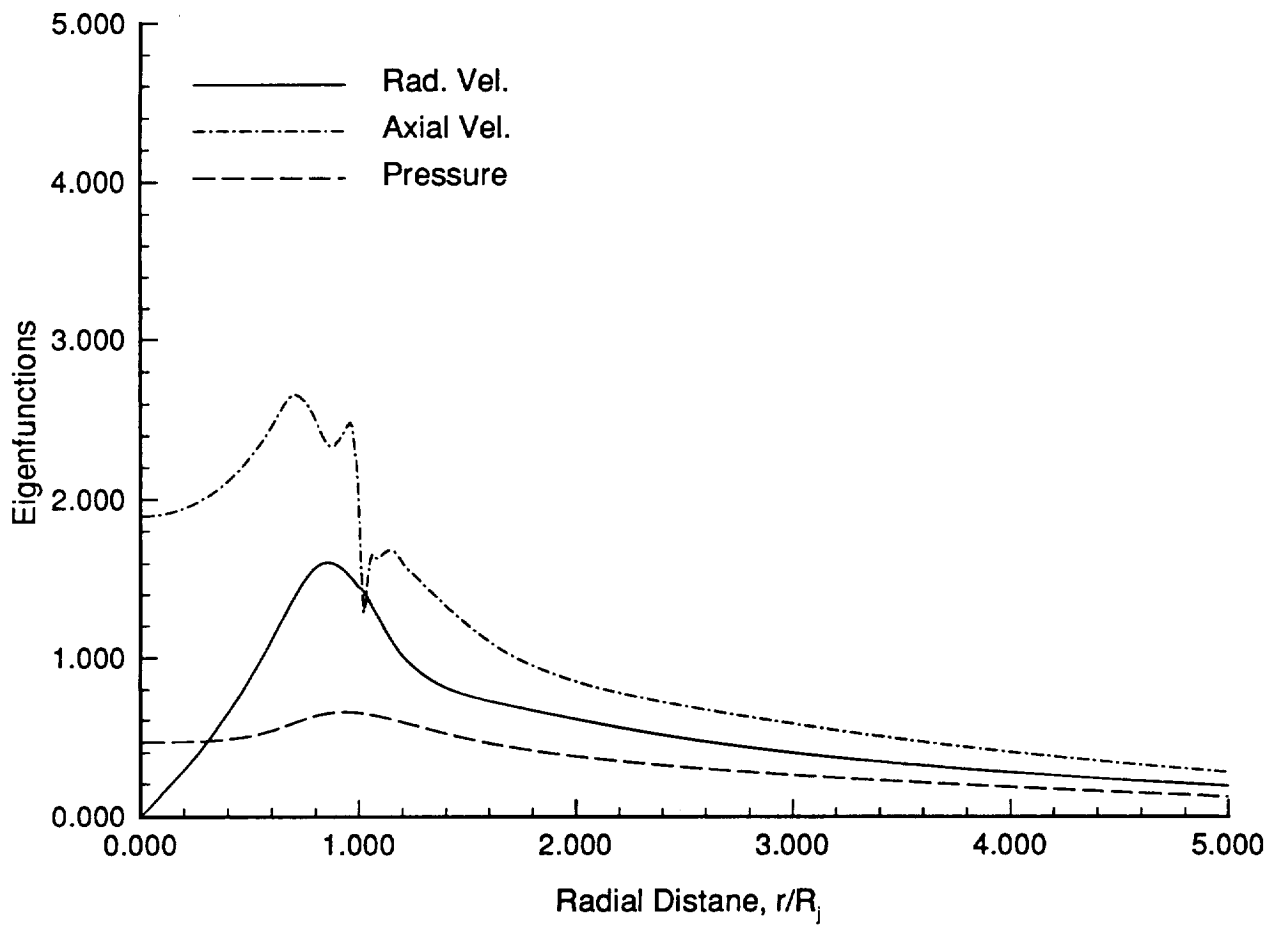Fig. 7. Eigenfunctions for $n = 0$, $St = 0.54$ at $X/R_j = 0$.

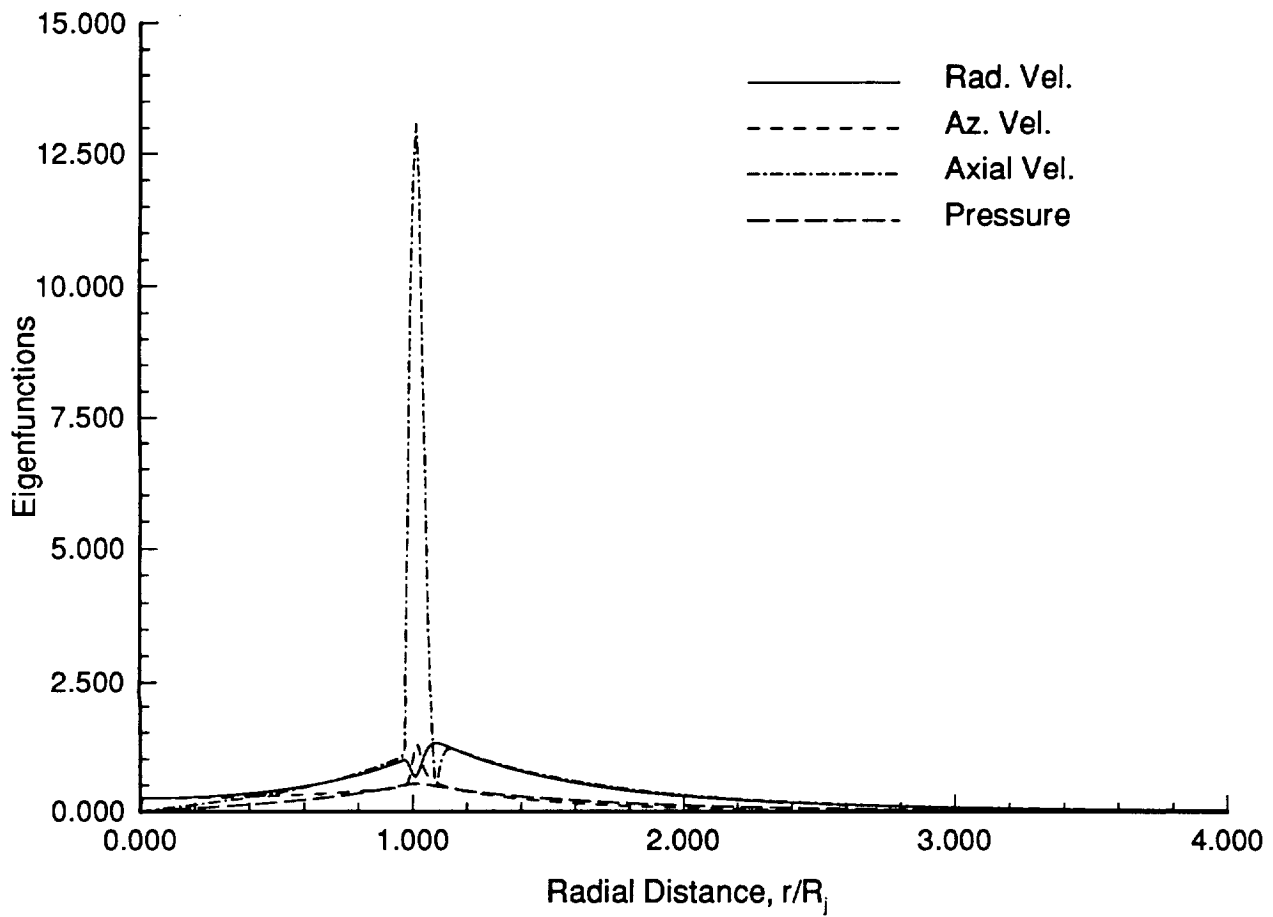Fig. 8. Eigenfunctions for $n = 0$, $St = 0.54$ at $X/R_j = 10$.

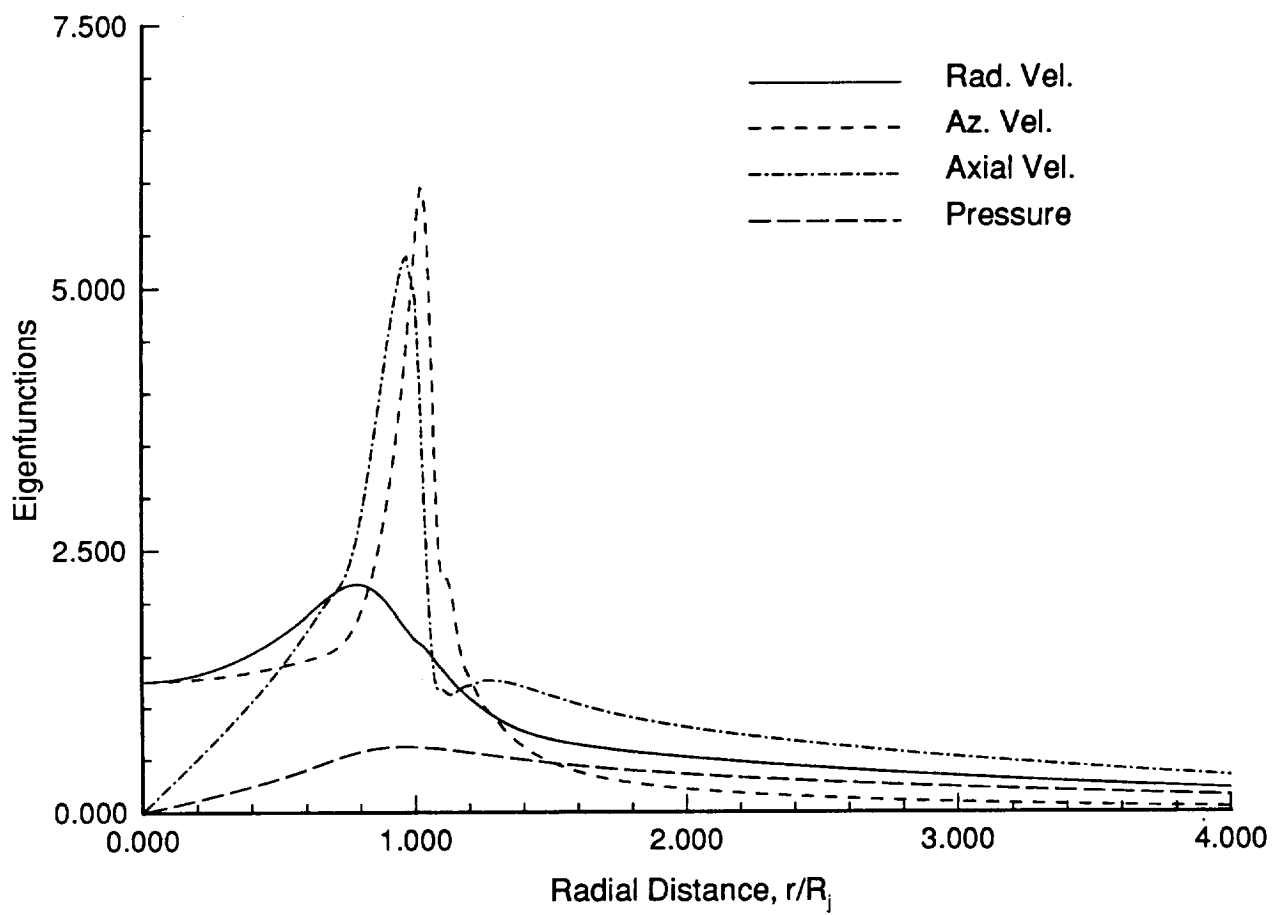Fig. 9. Eigenfunctions for $n = 1$, $St = 0.49$ at $X/R_j = 0$.

Fig. 10. Eigenfunctions for $n = 1$, $St = 0.49$ at $X/R_j = 10$.